Proceedings of the ASME 2010 3rd Joint US-European Fluids Engineering Summer Meeting and
8th International Conference on Nanochannels, Microchannels, and Minichannels
FEDSM-ICNMM2010
August 1-5, 2010, Montreal, Canada

FEDSM-ICNMM2010-31160

THERMOHYDRAULIC CHARACTERISTICS OF FLUID FLOW IN A ZIG-ZAG SQUARE MICROCHANNEL

B. Mathew
College of Engineering and Science
Louisiana Tech University
Ruston, LA 71272
bma017@latech.edu

T. J. John
College of Engineering and Science
Louisiana Tech University
Ruston, LA 71272
tomjj0579@gmail.com

H. Hegab
College of Engineering and Science
Louisiana Tech University
Ruston, LA 71272
hhegab@latech.edu

ABSTRACT

This paper deals with understanding the thermohydraulic characteristics of one type of zig-zag square microchannel. Studies are done to understand the individual effect of geometric parameters like hydraulic diameter, orientation angle and connector length for Reynolds number between 100 and 400. The hydraulic diameter is varied between 100 µm and 300 µm with increment of 100 µm. Studies are carried out for orientation angle of 10^{o}, 20^{o} and 30^{o}. The connector length of the study conducted in this paper is varied from 200 µm to 400 µm to 600 µm. The results are presented in terms of enhancement of Nusselt number and Poiseuille number over that in straight square microchannels. With increase in hydraulic diameter the enhancement in Nusselt number and Poiseuille number increased at a specific Reynolds number. Similarly with increase in the orientation angle the enhancement in these two thermohydraulic characteristics is observed for a specific Reynolds number. With increase in connector length both Nusselt number and Poiseuille number increased over that in straight channels of the same hydraulic diameter for a particular Reynolds number. Enhancement in Nusselt number and Poiseuille number is observed with increase in Reynolds number for all zig-zag microchannels. For the three fold increase in each of the geometric parameters the smallest enhancement is observed with increase in connector length. The greatest enhancement in thermohydraulic characteristics is observed with change in orientation between the arm and the connector.

INTRODUCTION

Enhancement of heat transfer coefficient in internal flows has always been of interest to the heat transfer community. The motivation behind enhancing heat transfer coefficient is the obvious reduction in size of the heat transfer device as well as residence time [1]. Several techniques are currently available for enhancing the heat transfer coefficient associated with heat transfer devices. All such techniques can be broadly classified into active and passive methods [2, 3]. Those techniques that require the use of external power to bring about the enhancement of heat transfer coefficient are referred to as active methods. On the other hand, techniques that do not require external power are classified as passive methods. One thing common to these existing techniques is that the manner in which the enhancement of heat transfer coefficient is achieved. These techniques bring about periodic disruption of the boundary layer and/or due to mixing of fluid across the cross section of flow [2, 3]. Thus the boundary layer in the channel is never fully developed. One of the latest methods for enhancing the heat transfer coefficient is through the use of nanofluids [4]. The presence of nanoparticles in these fluids increases the thermal conductivity of the fluid-nanoparticle mixture above that of the fluid itself is considered as the main reason behind the observed improvement of heat transfer coefficient. Thus this technique is based on the alteration of the thermophysical property of the fluid unlike the techniques already mentioned.

One of the motivations towards implementing microchannels in heat transfer devices is the possible enhancement of heat transfer coefficient. The heat transfer coefficient increases with reduction in channel size because the boundary layer thickness also reduces with reduction in channel size. Heat exchangers developed by Heatric®, Velocys, and Chart-Industries employ microchannels. This article details a passive method for bring about further increase in the heat transfer coefficient associated microchannels. Period disruption of the boundary layer and mixing is achieved by creating the microchannel in a zig-zag manner rather than as a straight channel. Thus whenever the flow changes direction the boundary layer get disrupted and this enhances the heat transfer coefficient. Moreover, the change in flow direction also brings about mixing of the fluid and this enhances the heat transfer coefficient as well. Alteration of flow direction in microchannels has been perceived as a means to enhance the heat transfer coefficient for almost a decade [5-7]. However, most attempts till date have focused on repeatedly altering the flow direction by 90^{o} [5, 6]. Such channels are aptly referred to as serpentine microchannels [5, 6]. The disadvantage with this approach is that the pressure drop associated with 90^{o} turns is extremely high, i.e. the cost to benefit ratio is very high. Secondly the use of serpentine microchannels brings about wastage of infrastructure. Therefore there is need for achieving balance between the certain constraints, i.e. maximizing heat transfer coefficient and minimizing the pressure drop and loss of infrastructure. The idea of zig-zag microchannels is born out of this need for balancing these constraints. Zig-Zag microchannels will bring about the desired enhancement in heat transfer coefficient but at the same time minimize pressure drop and loss of infrastructure. This article analyzes the thermofluidic performance of square zig-zag microchannels with respect to the hydraulic diameter, orientation and connector length for Re between 100 and 400.

NOMENCLATURE

A	: area (m^2)
C_p	: specific heat (J/kg K)
D_{Hy}	: hydraulic diameter (μm)
f	: friction factor
fRe=Po	: Poiseuille number
H	: constant heat flux thermal boundary condition
k	: thermal conductivity of fluid (W/m K)
L	: length of the straight microchannel that is transfored into zig-zag microchannel (μm)
l	: length of each arm of a repeating unit (μm)
Nu	: Nusselt number
P	: local pressure (kPa)
ΔP	: pressure drop (kPa)
Pr	: Prandtl number
q"	: parameter symbolizing heat flux
$\dot{q}$	: parameter symbolizing volumetric flow rate
Q	: volumetric flow rate (m^3/sec)
Re	: Reynolds number
T	: temperature (K)
u,v,w	: X, Y, Z component of the velocity vector (m/sec)
U	: average cross sectional velocity (m/sec)
V	: velocity vector (m/sec)
W	: width/height of the microchannel
X,Y, Z	: spatial coordinates
α	: thermal diffusivity (m^2/sec)
θ	: arm angle (orientation of each arm of the repeating unit with the X-axis)
μ	: viscosity (Pa.s)
ρ	: density (kg/m^3)

Subscripts

avg	: average
cr	: cross section
f	: fluid
in	: inlet
out	: outlet
r	: relative
w	: wall

LITERATURE REVIEW

Chintada et al. [5] numerically studied the behavior of Nu and fRe in a three dimensional serpentine channel with right angle turns. The channel is subjected to constant heat flux. Studies were carried out using both air and water for Re = 50, 100, 150 and 200. With increase in distance between two consecutive right angled turns the enhancement in fRe is observed with increase in Re for a channel with specific hydraulic diameter. This enhancement in fRe is observed for both air and water. On the other hand, no enhancement in Nu is observed for air with increase in the distance between two consecutive right angled turns for Re = 50 and100. In fact, the Nu for such cases is smaller than that in straight channels. For Re = 150, enhancement in Nu is observed in certain cases studied with respect to the distance between two consecutive right angled turns; while for Re = 200 enhancement in Nu is observed for all cases. However, for water enhancement in Nu is observed for all values of Re irrespective of the distance between two consecutive right angled turns.

Geyer et al. [6] studied the enhancement in Nusslet number and Poiseuille number in a planar serpentine square microchannel subjected to constant heat flux (H2 condition) as well as constant temperature for Re lower than 200. The effect of geometric parameters on the Nu and fRe is analyzed in this paper. These authors also studied the effect of Pr on the enhancement in Nu and fRe. With increase in Re the enhancement in Nu and fRe increased. The enhancement in Nu is greater than that of fRe. With increase in Pr the enhancement in Nu increased when the serpentine microchannel is subjected to constant heat flux. For air, Nu increased for all values of Re. This is in direct contradiction to that observed by Chintada et al. [5]. With increase in length between each turn (90^{o}) the overall enhancement in Nu and fRe decreased for a specific Re, Pr and hydraulic diameter.

Gupta et al. [7] studied the enhancement in Nu and fRe of a zig-zag triangular microchannel for Re ≥ 200. The thermohydraulic characteristics of microchannels with triangular cross section are compared with similar microchannels with cross sections like square, semi-circle, and circle. The best overall performance, defined as the ratio of enhancement in Nu over enhancement in *f*Re, is for microchannels with triangular cross section for the above mentioned Re. With increase in connector length the enhancement in Nu and *f*Re for zig-zag microchannels with triangular and semi-circular cross section increased for a specific Re. The enhancement in Nu is the lowest when the microchannel profile is that of an equilateral triangle. The enhancement in Nu increases when the apex angle is different from 60^o.

From the brief review of literature provided here it is clear that there is currently no study available on zig-zag square microchannels. Subsequently the thermohydraulic characteristics of such microchannels are studied in this paper.

THEORETICAL MODEL

Figure 1 is a schematic of the repeating unit of a zig-zag microchannel that is studied in this paper. The repeating unit consists of two arms that are joined to a straight microchannel also referred to as connector in this article. The arms are of equal length and oriented at an angle (θ) with respect to the connector. Both the arms are oriented equally with respect to the connector. Total length of the repeating unit is the sum of the length of two arms and two connectors. Prior to developing the governing equations describing the flow in the microchannel certain assumptions are made in order to the ease the modeling process. These assumptions are provided below.

1. Only the steady state condition of the flow in the microchannel is analyzed.
2. The repeating unit used for the thermofluidic analysis is far from the inlet and outlet of the microchannel.
3. The walls of the microchannels are perfectly smooth.
4. No-slip boundary condition is assumed on the microchannel walls.
5. Effect such as external heat loss, internal heat generation, axial heat conduction, flow maldistribution and viscous dissipation are neglected.
6. Phase change does not occur for the fluid within the microchannel.

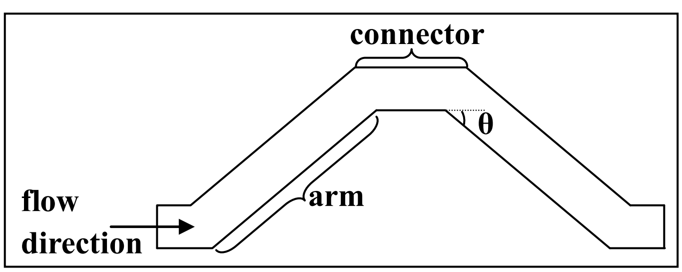

Figure 1: Drawing of a repeating unit of the zig-zag microchannel studied in this paper.

Assumption 2 states that the repeating unit that is used for analyzing the thermophysical characteristics in this study is far from the inlet and outlet of the microchannel. This is done in order to prevent the influence of entrance effects due to the entry of flow from the manifold to the microchannel on Nu and *f*Re. This entrance effect would be present just in the repeating units nearest to the entrance of the microchannel and has to be avoided while analyzing the observed thermofluidic characteristics.

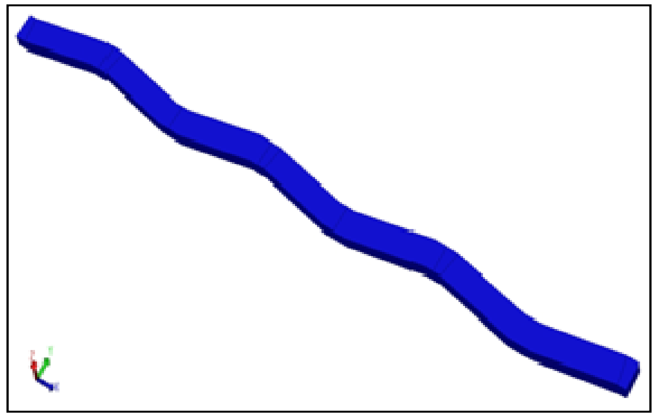
Figure 2: Schematic of the zig-zag microchannel analyzed in this article.

Based on these assumptions the governing equations for the microchannel are formulated and provided below. Equation (1) is the continuity equation while the three momentum equations (in vector form) are provided in Eq. (2). The energy equation of the fluid is presented in Eq. (3). The heat transfer through the wall of the microchannel is not of interest in this study and thus neglected. Thus only the liquid occuping the microchannel is used for purposes of analysis. Therefore the term microchannel just refers to this body of fluid in this study. The heat flux is applied on the outer surface of the microchannel. The term wall is used in this study for referred to the outer surface of the microchannel.

Continuity Equation

$$\nabla \cdot \vec{V} = 0 \tag{1}$$

Momentum Equation

$$\vec{V} \cdot \nabla \vec{V} = -\nabla p + \mu \nabla^2 \vec{V} \tag{2}$$

Energy Equation (fluid)

$$\vec{V} \cdot \nabla T = \alpha \nabla^2 T \tag{3}$$

Several boundary conditions are required to solve this set of governing equations. The momentum equation is second order in all the three directions and thus two boundary conditions are required for Eq. (2). The associated boundary conditions are provided in Eqs. (4) - (6).

$$\dot{Q}_{in} = q \tag{4}$$

$$u_{wall} = v_{wall} = w_{wall} = 0 \quad (5)$$

$$p_{out} = 0 \quad (6)$$

Equation (4) represents the flow rate at the inlet to the microchannel. Even though the momentum equation is in terms of the velocity it is acceptable to provide volumetric flow rate as a boundary condition at the inlet to the microchannel. CoventorWare™ will calculate the velocity normal to the cross sectional area of flow based on this volumetric flow rate (Q_{in}) and the geometric parameters of the microchannel. The parameter Q_{in} represents the volumetric flow rate while the parameter $\dot{q}$ is the symbolic representation of the value of volumetric flow rate. If the inlet cross section is aligned along any one of the axes then the velocity thus calculated will be assigned to the velocity component along that axis and the velocities in the other two directions will be taken to be zero. On the other had if the cross section is aligned at an angle with respect to the coordinate axis then the velocity thus calculated is the resultant of the velocities in three directions and it would be resolved to obtain each component of velocity. For the model developed in this paper the normal to the cross sectional area at the inlet is aligned along the X-direction. Thus the velocity determined using the volumetric flow rate is equal to that in the X-direction. The velocities in the other direction are taken to be zero at this section. The second boundary condition of the momentum equation is based on the no-slip boundary condition as well as on the fact that the wall is impermeable. Thus the velocity normal to the wall is zero as the wall is impermeable and the velocity tangential to the wall is also zero as the no-slip boundary condition is imposed on it. The boundary condition at the exit of the microchannel is provided in Eq. (6). The pressure and velocity is coupled through the momentum equation and thus the pressure specified at this boundary is used as the boundary condition of the momentum equations. In order to ease the computation process the pressure at the outlet of the microchannel is forced equal to zero. As this study requires only pressure drop rather than absolute pressure, the act of assigning pressure at the outlet of the microchannel will not alter the calculations. At this stage it has to be remembered that in real situations the pressure at the outlet will only be equal to zero if the flow has to be stopped at that location.

The energy equation (Eq. (3)) of the microchannel is second order in all directions, thus two boundary conditions are required in all the three directions to solve this equation. The boundary conditions associated with the energy equations are provided in Eq. (7), Eq. (8) and Eq. (9). Equation (7) is the mathematical representation of the heat flux imposed on the wall of the microchannel. Like before q_{wall} is the parameter representing the heat flux on the wall and q'' symbolizes the value that is assigned to q_{wall}. As seen in Fig. 1 the microchannel dealt with in this study is horizontal with the bottom surface aligned on the X-Y plane passing through Z = 0. The boundary condition in the Z-direction for every repeating unit would be the heat flux applied on the top and bottom of the microchannel. The heat flux applied at the top and bottom of the microchannel is equal to q''. On the other hand the boundary condition of all repeating units in the Y-direction is equal to the heat flux in the direction normal to the right and left wall of the microchannel, i.e. the component of q'' normal to the right and left wall. The inlet temperature of the fluid is always a known parameter and it is used as one of the boundary conditions in the X-direction. For this study the temperature at the inlet section of the microchannel is taken to be equal to 273.15 K (Eq. (8)). A second boundary condition in the X-direction is required to complete the thermal model. For this the outlet section of the microchannel is assumed to be insulated. This is mathematically represented as shown in Eq. (10).

$$\left.\frac{\partial T}{\partial \vec{n}}\right|_{wall} = q'' \quad (7)$$

$$T_{in} = 273.15K \quad (8)$$

$$\left.\frac{\partial T}{\partial X}\right|_{out} = 0 \quad (9)$$

For both the momentum and energy equation the boundary condition in the X-direction is defined at the ends of the microchannel and not just at the ends of the repeating unit. This is because the temperature and velocity profile of the entire microchannel is solved every time and the results of the desired repeating unit extracted from it.

In one of the earlier sections it is mentioned that the study is performed for Re between 100 and 400 with increment of 100. Based on the desired Re and the geometry of the microchannel the volumetric flow rate is calculated as shown in Eq. (10). The value of volumetric flow rate thus calculated is used as an input to CoventorWare™.

$$\dot{q} = \frac{\mu \operatorname{Re} A_{cr}}{\rho D_{Hy}} \quad (10)$$

The heat flux also needs to be supplied as an input parameter for solving the system of equations presented above. For this study it is desired that every repeating unit of the microchannel absorb 1 W of heat. Thus heat flux is determined using the heat input to the repeating unit as well as its surface area.

CoventorWare™ is a CFD software package specifically for microfluidic applications. CoventorWare™ solves CFD problems using control volume approach using the PISO algorithm. CoventorWare™ solves a steady state problem as an unsteady state problem. The iteration is carried out till the solutions (velocities and temperature) become independent of time. Upwind scheme is used for discretize the convective terms. The fact that the zig-zag microchannel has irregular boundaries, though periodically repeating, prevents users of CoventorWare™ from meshing this computational domain using regular cuboid shaped control volumes. However, CoventorWare™ allows users to mesh irregular geometries like zig-zag mircochannel using a specialized mesh setting called 'extruded mesh'. While using extruded mesh CoventorWare™ initially meshes the bottom surface, i.e. the surface aligned with the X-Y plane passing through Z=0 of the microchannel and then extrudes this surface mesh in the third direction (Z-direction) to form a three dimensional control volume. CoventorWare™ lets users control the dimensions of the control volume. For the studies conducted in this article the two widths of the surface mesh is maintained 6-15 micrometers while that in the extruded direction is kept between 3-7 micrometers. The relative convergence criteria for the discretized momentum equations are kept equal to 10^{-4}. The relative convergence criterion for the energy equation is maintained at 10^{-7}. The error associated with the source term of the continuity equation is maintained at 10^{-4}. This is the default setting of CoventorWare™, but can be changed based on the discretion of the user. The grid independency on the results is validated by carrying out simulations for a specific model, i.e. specific geometry and input parameters, using different mesh settings. With each refinement of mesh settings the number of nodes/control volume associated with the computational domain is increased. The refinement of mesh is carried out till until two criteria are satisfied. The first criterion is the matching of volumetric flow rate at the inlet and outlet of the desired repeating unit with that at the inlet of the microchannel. This criterion is assumed to be satisfied when the percentage difference between the flow rate at the inlet of the microchannel and that the inlet and outlet of the desired repeating unit is between 1-2%. CoventorWare™ has the provision for determining the flow rate at any desired cross section based on the solution of the momentum equation, i.e. velocities. The second criterion is on the temperature at the inlet and outlet sections of the desired repeating unit. If the change in temperature at these sections is smaller than 10^{-2} K then this criterion is satisfied.

Based on the average temperatures of the fluid and wall at a section of a repeating unit it is possible to determine the average heat transfer coefficient of that particular section. The average heat transfer coefficient at that section is determined based on Eq. (11). Average heat transfer coefficient of the entire repeating unit is determined using the average heat transfer coefficients at different three sections of the repeating unit. Two of these sections are the inlet, and the outlet of the repeating unit. The third section is the mid point of the connector of a repeating unit. Based on the average heat transfer coefficient it is possible to determine the average Nusselt number at a section using Eq. (12).

$$h_{avg} = \frac{q^{"}}{(T_{w,avg} - T_{f,avg})} \tag{11}$$

$$Nu_{avg} = \frac{h_{avg} D_{hy}}{k_f} \tag{12}$$

The other quantity of interest in this study is the Poiseuille number. Prior to determining the Poiseuille number it is important to determine the friction factor (*f*). Friction factor is determined based on the pressure drop between the inlet and outlet of the repeating unit using Eq. (13). Based on *f* the Poiseuille number can be determined as shown in Eq. (14). The Poiseuille number thus determined would be the average in the repeating unit.

$$f = 2\frac{\Delta P D_{Hy}}{\rho U^2 L} \tag{13}$$

$$Po = f\,\mathrm{Re} \tag{14}$$

It has been mentioned earlier than the purpose of using zig-zag microchannels instead of straight one is for enhancing the heat transfer coefficient. Therefore the relative improvement in heat transfer coefficient is of great interest to the designer. The relative increase in Nu is calculated based on Eq. (15). The denominator represents the Nu for a square channel under fully developed flow condition. Due to the change in flow direction the Poiseuille number will also be higher in a zig-zag microchannel in comparison with a straight microchannel. The relative increase in Poiseuille number relative to that of a straight microchannel under fully developed flow condition is determined using Eq. (16).

$$Nu_r = \frac{Nu_{zig-zag}}{Nu_{straight}} \tag{15}$$

$$\left(f\,\mathrm{Re}\right)_r = \frac{(f\,\mathrm{Re})_{zig-zag}}{(f\,\mathrm{Re})_{straight}} \tag{16}$$

RESULTS AND DISCUSSION

CoventorWare™ is initially used for determining the Nu and *f*Re in a square straight microchannel of size 200 by 200 micrometers. The results obtained from this exercise are compared with that available in literature [8]. This is done in order to validate the model as well as the numerical schemes used by ConventorWare™. The results matched very well with that available in literature thereby proving the validity of the mathematical scheme and the equations defining the model [8].

Figure 3 is a contour plot of the velocity in a zig-zag microchannel. The microchannel consists of a few set of repeating uinits. This figure will provide a better understanding of the second assumption made while developing this model.

From this figure it can be clearly seen that at the entrance of the microchannel the flow is affected by entrance effects that is present due to the movement of fluid from the manifold to the microchannel. The third repeating unit is used in this study for analyzing the thermofluidic characteristics. In this way no influence of the entrance effects at the inlet of the microchannel is included in measured thermofluidic characteristics of the zig-zag microchannel.

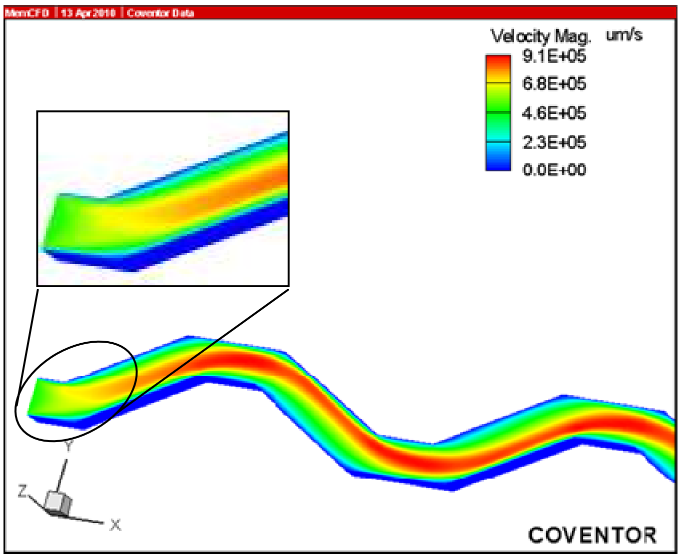

Figure 3: Contour plot of velocity at the mid-section of the zig-zag microchannel showing entrance effect (Re = 100, D_{Hy} = 300 μm, θ =30°)

Figure 4 and Fig. 5 represents the effect of hydraulic, for Re varying between 100 and 400, on the Nu_r and $(f\mathrm{Re})_r$, respectively. The hydraulic diameter is varied between 100 μm and 300 μm with increment of 100 μm. The orientation between each of the arms and the connector is kept at 10°. It can be seen from these figures that Nu_r and $(f\mathrm{Re})_r$ is greater than unity for a specific Re irrespective of the hydraulic diameter. This is because the zig-zag nature of the microchannel leads to mixing as well as disruption of the boundary layer at the locations where there is change in flow direction. Mixing characteristics of zig-zag microchannels has been studied previously by researchers [9]. Mixing mainly occurs due to change in flow direction. Whenever flow direction changes secondary flow is introduced in the plane normal to the flow direction. The change in flow direction associated with the zig-zag microchannels shown in Fig. 1 and Fig. 2 would be between each arm and the connector of a repeating unit. The mixing of the fluids reduces the temperature of the fluid adjacent to the wall which in turn helps reduce the temperature of the wall at that location. When the flow direction changes, i.e. at the intersection between each arm and the connector, the boundary layer is disrupted due to flow separation. From Fig. 6 it can be seen that the flow separation mainly occurs at the when the flow moves past the intersection between the connector and arm. This is because the velocity is skewed towards the outer wall as the flow reaches the intersection between the connector and the arm. On the other hand, flow separation is not observed as flow moves past the intersection between the arm and the connector because the velocity is skewed towards the inner wall. Occurrence of flow separation is show in Fig. 6. This disruption of the boundary layer helps reduce the thermal resistance between the wall and the fluid and in turn provides additional help in reducing the wall temperature. This reduction in wall temperature due to mixing and boundary layer disruption leads to increase in Nu and thus the observed increase in Nu_r. The cross-sectional area normal to the flow in the connector is smaller than that of the arm of the microchannel. Thus when the flow moves between the arm and the connector there is either constriction or expansion of the flow area. This plays to increases the severity associated with mixing and disruption of boundary layer along with that due occurring due to change in flow direction. Though both mixing and disruption of the boundary layer has positive effect on heat transfer these phenomena have an adverse effect on pressure drop. Mixing of the fluid leads to increase in pressure drop. The change in flow direction and the constriction/expansion of flow area which causes disruption of boundary layer is also involved in increasing the pressure drop. Thus mixing and boundary layer disruption present in each repeating unit of the zig-zag microchannel acts to increase the Poiseuille number as seen in Fig. 5.

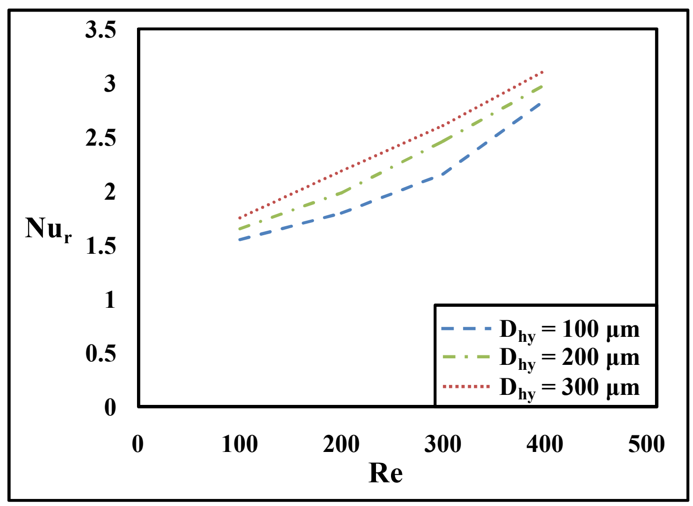

Figure 4: Variation of Nu_r with Re and D_{Hy} (θ = 10°)

It can also be seen from these figures that with increase in Re both Nu_r and $(f\mathrm{Re})_r$ increased irrespective of the hydraulic diameter. With increase in Re the flow rate increases as the hydraulic diameter is kept constant. With increase in flow rate the degree of mixing increases within each of the repeating unit. The increased mixing leads to greater reduction of the temperature of the fluid adjacent to the walls. This in turn helps decrease the wall temperature. Moreover with increase in flow rate in a specific microchannel the momentum associated with the flow increases. This increase in the momentum of the flow leads to greater degree of flow separation at the intersection between the arms and connectors which in turn causes the disruption of the boundary layer also gets more severe. This too has a positive effect on the thermal resistance between the wall and the fluid. These two effects act to increase Nu_r with increase in Re. In addition to the increase in Nu_r with Re the Poiseuille number also increases with increase in Re. The increase in $(f\mathrm{Re})_r$ is also due to increased mixing and greater disruption of boundary layer.

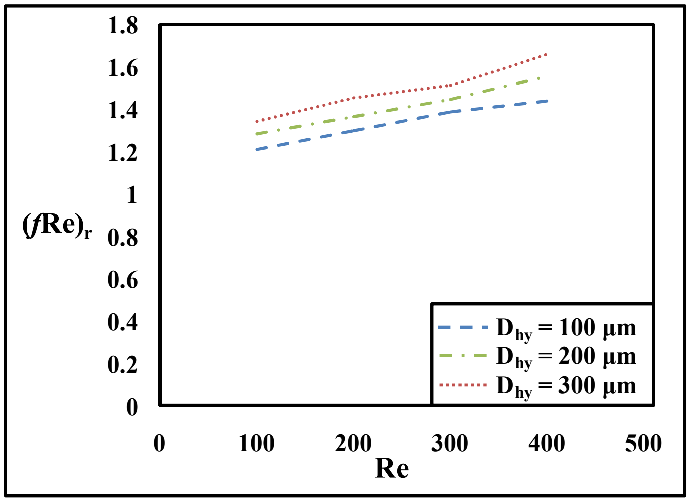

Figure 5: Variation of $(f\mathrm{Re})_r$ with Re and D_{Hy} ($\theta = 10^o$)

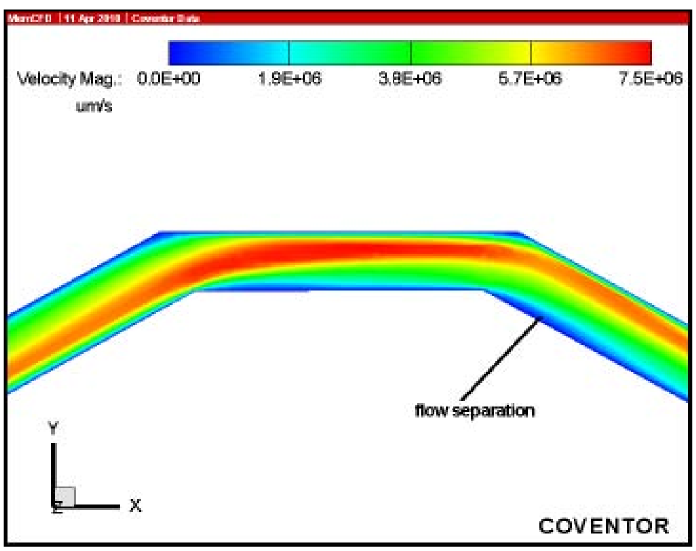

Figure 6: Velocity contour plot of the connector at the mid-sectionof zig-zag microchannel (Re = 300, D_{Hy} = 100 µm, $\theta = 10^o$)

The parameters Nu_r and $(f\mathrm{Re})_r$ increase with increase in hydraulic diameter. This has been observed by previous researchers as well [5-7]. When the hydraulic diameter is increased at a specific Re it is necessary to increase the flow rate. However the heat input to each repeating unit is maintained constant and thus the temperature rise of the fluid reduces. This reduced temperature of the fluid helps lower the wall temperature and increase Nu with increase in hydraulic diameter.

The influence of the angle between each arm and the connector is studied in Fig. 7 and Fig. 8. The zig-zag microchannel considered studied in these figures has hydraulic diameter of 200 µm. The orientation between each arm and the connector is varied between 10^o to 20^o to 30^o. The total length of the repeating unit of the zig-zag microchannel is kept constant at 2400 µm.

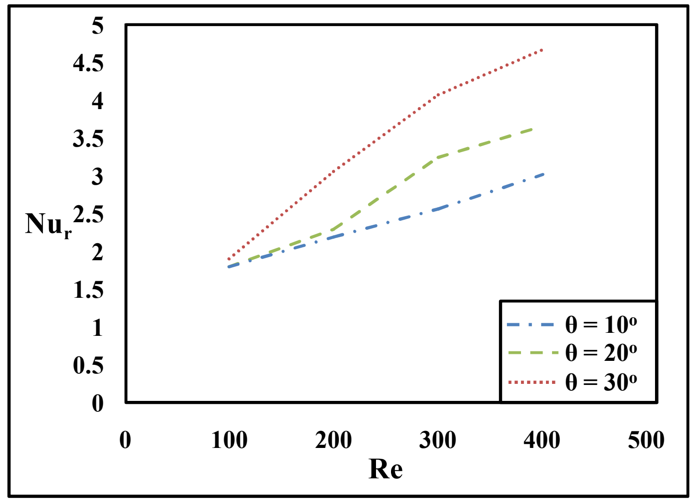

Figure 7: Variation of Nu_r with Re and θ (D_{Hy} = 200 µm)

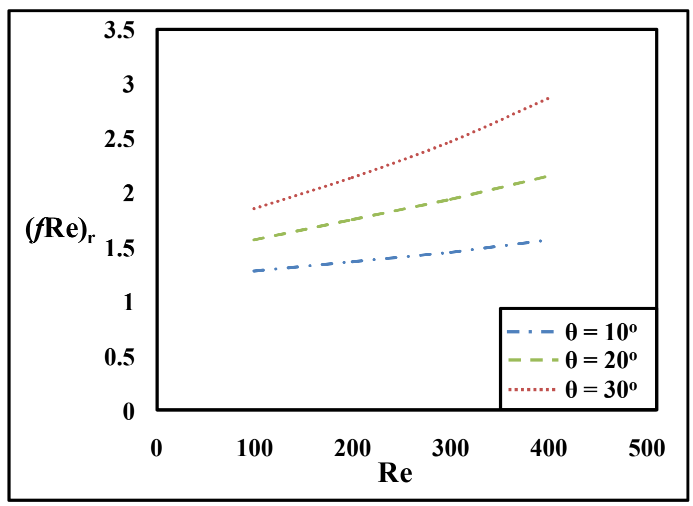

Figure 8: Variation of $(f\mathrm{Re})_r$ with Re and θ (D_{Hy} = 200 µm)

With increase in θ, Nu_r and $(f\mathrm{Re})_r$ increased at a specific Re. This is because with increase in θ the change in flow direction that takes place whenever flow moves from an arm to the connector or vice versa of a repeating unit increases. This leads to increased mixing at the intersection between the arm and the connector of the zig-zag microchannel. This acts to enhance the Nu and fRe associated with the zig-zag microchannel at a specific Re. Also the increase in orientation between an arm and a connector will bring about greater disruption of the boundary layer which too helps reduce the thermal resistance between the wall and the fluid to enhance Nu. This can be observed by comparing the velocity contour plots shown in Figs. 9-10. With increase in orientation the degree of flow separation increases. Flow separation occurs as the flow moves past the intersection between the connector and the arm. The disruption of the hydrodynamic boundary layer at the intersection between each arm and the connector also acts to increase pressure drop greater than that in a straight microchannel with the same hydraulic diameter. Moreover, this mixing and disruption of boundary layer gets more severe with increase in orientation. This is because with increase in orientation the hydraulic diameter of the connector reduces. Reduction in hydraulic diameter of the connector leads to reduction in flow area. Therefore for a specific flow rate, associated with a specific Re and hydraulic diameter, greater the change in flow area higher the severity associated with mixing and disruption in boundary layer and thus the observed increase in Nu_r and $(f\mathrm{Re})_r$ with increase in orientation for a specific Re.

From these figures it can be noticed that with increase in Re the parameter Nu_r and $(f\mathrm{Re})_r$ increased. The reason for this is same as that already explained earlier.

The effect of connector length is also investigated in this study. The connector length is varied between 200 µm and 600 µm for a zig-zag microchannel of hydraulic diameter of 200 µm. The total length of reach repeating unit of the microchannel is kept at 2400 µm. When the length of the connector is 400 µm then the length of each is 1000 µm. If the connector length is 600 µm then the sum of the lengths of the arms is 1800 µm. The orientation between each of the arms and the connector is maintained at 10^o when the connector length is 200 µm. Figure 12 and Fig. 13 represents the variation of Nu_r and $(f\mathrm{Re})_r$ with Re for the above mentioned microchannels.

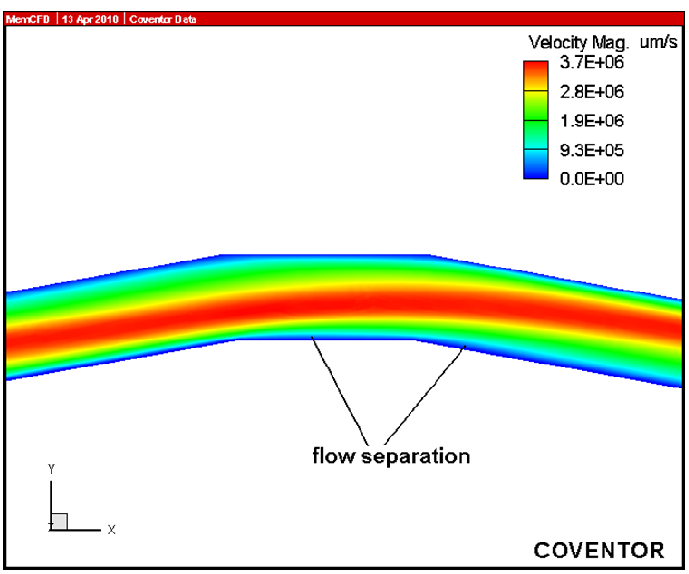

Figure 9: Contour plot of velocity showing flow separation in a zig-zag microchannel (Re = 300, D_{Hy} = 200 µm, $\theta = 10^o$).

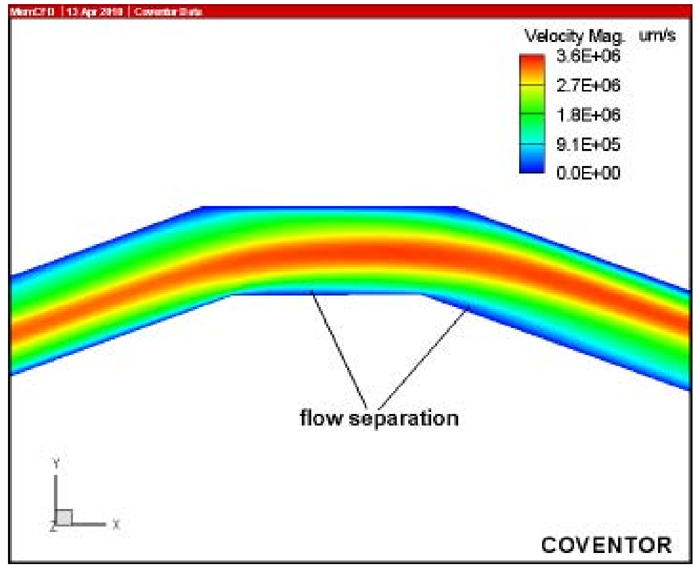

Figure 10: Contour plot of velocity showing flow separation in a zig-zag microchannel (Re = 300, D_{Hy} = 200 µm, $\theta = 20^o$).

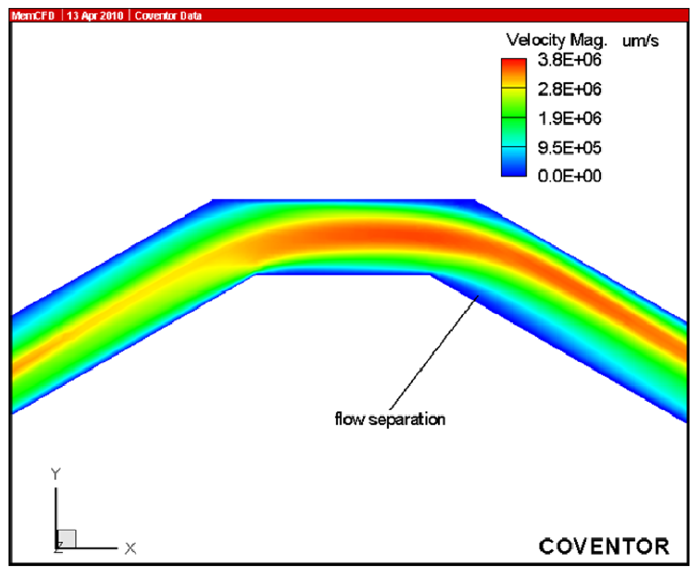

Figure 11: Contour plot of velocity showing flow separation in a zig-zag microchannel (Re = 300, D_{Hy} = 200 µm, $\theta = 30^o$).

From these figures it can be seen that with increase in connector length the parameter Nu_r increased. Gupta et al. [8] too observed such a trait in triangular and semi-circular zig-zag microchannels. For the cases considered here the change in flow direction increases with increase in connector length. This is because the distance between the mid-section of one connector to that o the next is kept constant in all the three cases studied here. Thus the degree of mixing brought about by the change in flow direction is not equal for the cases analyzed here. It increases with increase in connector length and is highest for the zig-zag microchannel with the connector length of 600 µm. Also the disruption and the redevelopment of boundary layer that occur are different in each of these cases.

This is because the disruption and redevelopment of the boundary layer that takes place in a zig-zag microchannel depends on the orientation and the length of the arms. The effect of the disruption and redevelopment of the boundary layer will be highest for the connector with length of 600 μm. The boundary layer that is disrupted at the intersection between the connector and arm will try to redevelop immediately in the arm that follows the intersection. The degree of redevelopment of the boundary layer that takes place in each arm depends on the length of the arm. Greater the length of the arm higher will be the degree of redevelopment. Thus the redevelopment will be highest in the zig-zag microchannel with the connector length equal to 200 μm. With the redevelopment of the boundary layer the thickness of the boundary layer increases and this increases the thermal resistance between the wall and the fluid. Lower degree of mixing and greater redevelopment of the boundary layer are the main reasons for the observed decrease in Nu_r and $(f Re)_r$ with reduction in connector length. For the connector with length of 200 μm the orientation is kept at 10^o as this is considered as the basic design. For the different connector lengths considered in this study the orientation increases but the increase is minor. As mixing and disruption/redevelopment of boundary layer depends on the orientation the minor increase in orientation brings about only minor increase in Nu_r and $(f Re)_r$ with change in connector length as observed in Figs. 12 and 13.

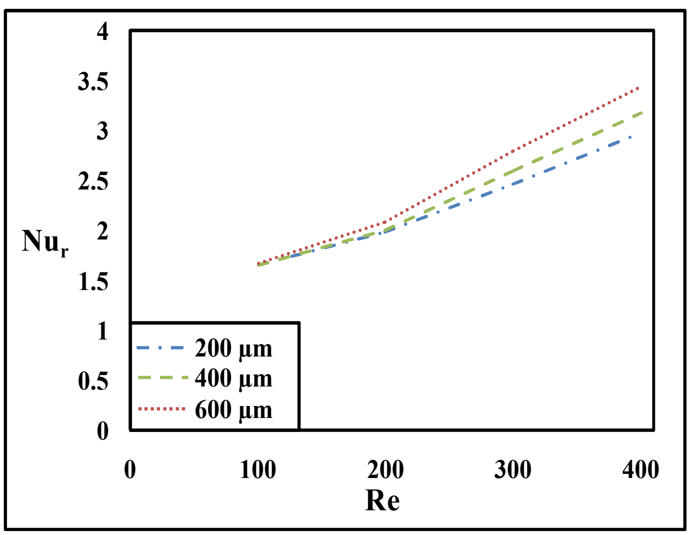

Figure 12: Variation of Nu_r with Re and connector length (D_{Hy} = 200 μm)

Similar to trend observed in the two previous cases, increase in Re increases Nu_r and $(f Re)_r$ irrespective of the connector length. The reason for this same as that mentioned earlier.

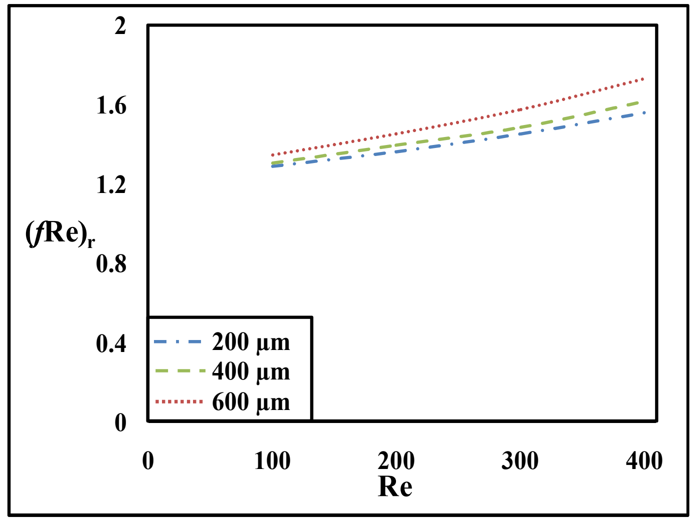

Figure 13: Variation of $(f Re)_r$ with Re and connector length (D_{Hy} = 200 μm)

CONCLUSION

The effect of geometric parameters of a zig-zag microchannel is analyzed in this paper for Re between 100 and 400. The results of this study are presented in terms of the ratio of Nusselt number and Poiseuille number of a zig-zag microchannel to that in a straight microchannel. Greater the ratio of Nusselt number better the thermal performance and higher the Poiseuille number worse the hydrodynamic characteristics. With increase in hydraulic diameter the ratio of both Nusselt number and Poiseuille number increased. On the other hand with increase in the orientation between the connector and each arm of the microchannel the ratio of Nusselt number and Poiseuille number increased. The effect of connector length was also investigated in this study and it is found that with increase in connector length enhancement in Nusselt number and Poiseuille number occurs. The greatest enhancement in both these parameters is observed with variation in orientation and the least enhancement occurs with changes in connector length.

REFERENCES

[1]. A. E. Bergles, 1997, Heat Transfer Enhancement – The Encouragement and Accomodation of High Heat Fluxes, Journal of Heat Transfer, vol. 119, pp. 8-19.

[2]. D. Westphalen, K. Roth, and J. Brodick, 2006, Heat Transfer Enhancement, ASHRAE Journal, vol. 48, pp.68-71.

[3]. M. E. Steinke, and S. G. Kandlikar, 2004, Single-Phase Heat Transfer Enhancement Techniques in Microchannel and Minichannel Flows, 2004 ASME International Conference on Microchannels and Minichanels, Rochester, NY, USA, June 17-19, pp.141-148.

[4]. X-Q. Wang, and A. S. Mujumdar, 2007, Heat Transfer Characteristics of Nanofluids: A Review, International Journal of Thermal Sciences, vol. 46, pp. 1-19.

[5]. S. Chintada, K-H. Ko, and N. K. Anand, 1999, Heat

Transfer in 3-D Serpentine Channels with Right-Angle Turns, Numerical Heat Transfer, Part A: Applications, vol. 38, pp. 781-806.

[6]. P. E. Geyer, N. R. Rosaquti, D. F. Fletcher, and B. S. Hayes, 2006, Thermohydraulics of Square-Section Microchannels Following a Serpentine Path, Microfluidics and Nanofluidics, vol. 2, pp. 195-204.

[7]. R. Gupta, P E. Geyer, D. F. Fletcher, B. S. Haynes, 2008, Thermohydraulic Performance of a Periodic Trapezoidal Channel with a Triangular Cross-Section, International Journal of Heat and Mass Transfer, vol. 51, pp. 2925-2929.

[8]. S. Kakac, 1987, Handbook of Single Phase Convective Heat Transfer, Wiley.

[9]. V. Mengeaud, J. Josserand, and H. H. Girault, 2002, Mixing Processes in a Zigzag Microchannel: Finite Element Simulations and Optical Study, Analytical Chemistry, vol. 74, pp. 4279-4286.